

Synthesis, Characterization, and Derivatization of Hyperbranched Polyfluorinated Polymers

Anja Mueller, Tomasz Kowalewski,[†] and Karen L. Wooley*

Department of Chemistry, Washington University, One Brookings Drive, Campus Box 1134, St. Louis, Missouri 63130-4899

Received August 7, 1997; Revised Manuscript Received November 6, 1997

ABSTRACT: A hyperbranched polyfluorinated benzyl ether polymer was prepared from the A₂B monomer 3,5-bis[(pentafluorobenzyl)oxy]benzyl alcohol. The polymerization was based upon deprotonation of the benzylic alcohol (B), followed by nucleophilic substitution of the *p*-fluorines of the two pentafluorophenyl (A) groups to form tetrafluorophenyl benzyl ether linkages. Optimized reaction conditions for the polymerization involved the addition of sodium metal (<0.1 mm particle size, 30 wt % suspension in toluene) to a solution of monomer (0.3 M) in THF heated at reflux. The molecular weight and molecular-weight distribution of the resulting polymer were affected by the surface area of the sodium particles, the concentration of the monomer, and the polymerization temperature. An average of one pentafluorophenyl chain end per repeat unit plus one pentafluorophenyl end group was present within the hyperbranched polymer, which allowed for chemical modification by nucleophilic displacement reactions upon the *p*-fluorines, to alter the physical and chemical properties of the material. Reaction of lithium trifluoroethoxide and lithium 1*H*,1*H*,2*H*,2*H*-perfluorodecanoxide with the pentafluorophenyl-terminated hyperbranched polymer introduced fluoroalkyl groups. Additionally, an X-ray opaque derivative was prepared by reaction of the pentafluorophenyl-terminated hyperbranched polymer with *p*-iodophenol. Contact angle measurements of water (96°, 99°, and 120°) and hexadecane (21°, 14°, and 62°) on films of a pentafluorophenyl-terminated hyperbranched polymer and the trifluoroethoxy-substituted and 1*H*,1*H*,2*H*,2*H*-perfluorodecanoxy-substituted derivatives, respectively, indicated a high degree of hydrophobicity and lipophobicity. Surface morphologies and surface properties of films were studied with atomic force microscopy (AFM). Tapping mode AFM images suggested phase separation in partially 1*H*,1*H*,2*H*,2*H*-perfluorodecanoxy-substituted material. Lateral force AFM (LFM) demonstrated that 1*H*,1*H*,2*H*,2*H*-perfluorodecanoxy substitution of the hyperbranched polymer led to a more than 2-fold decrease in the coefficient of friction and adhesive force, as measured with a silicon nitride probe.

Introduction

The field of study involving highly branched polymers has seen an explosion of interest in the past few years,¹ in all areas including theory, synthesis, characterization of structure and properties, and investigation of potential applications. Dendrimers have a well-defined structure and branching at each repeat unit, which imparts high solubility and low viscosity² for the materials, suggesting behavior that resembles that of "molecular ball bearings".³ Evidence for this model was shown in a recent study involving a combination of selective stable isotope labeling, rotational-echo double-resonance (REDOR) NMR, and molecular modeling for benzyl ether dendrimers.⁴ Recent Monte Carlo calculations on model dendrimers have supported segregation of dendron segments and inward-folding of the chain ends.⁵

The stepwise synthetic schemes required for the preparation of dendritic structures limit their accessibility. As an alternative, several hyperbranched polymers have been constructed of varying chemistries, by the direct condensation of A_xB monomers. The structure of hyperbranched polymers is not as controlled as that of dendrimers, with branching being random and less than 100%. Although the degrees of branching for dendrimers and hyperbranched polymers are very different, the overall composition is the same (when the

monomeric repeat units are the same).⁶ As a result, the properties for hyperbranched polymers lie between those found for linear and dendritic polymers.^{1c,7}

In the creation of low-surface-energy materials, fluorocarbons are often used.⁸ Fluorocarbons exhibit increased thermal stability, hydrophobicity and lipophobicity, and chemical resistance and decreased intermolecular attractive forces, in comparison to their hydrocarbon analogues.⁹ Fluorinated polymers¹⁰ have low cohesive and adhesive forces, low surface energy, high chemical resistance, and high thermal resistance, and most have low solubility. The properties that are responsible for the ability of fluoropolymers to perform as minimally adhesive and chemically resistant surfaces also contribute to the difficulties experienced in processing of the materials.

To merge these two systems and create materials with properties that resemble the physical properties of highly branched polymers (e.g. high solubility and low viscosity), in addition to the behavior found for fluoropolymers (e.g. hydrophobicity, lipophobicity, chemical resistance, and low cohesive forces), fluorocarbon units have been incorporated into the composition of hyperbranched polymers. Although reports of hyperbranched polymers containing fluorocarbon units have appeared,¹¹ the resulting effects upon the surface properties were not investigated. We report the synthesis and characterization of pentafluorophenyl-terminated hyperbranched benzyl ether polymers. Furthermore, the

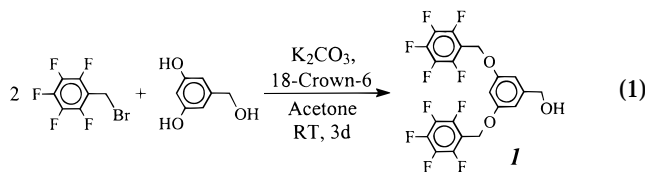
* Corresponding author.

[†] Corresponding author for AFM.

pentafluorophenyl terminal groups were employed for the introduction of perfluoroalkyl chains to increase the fluorocarbon character and generate highly fluorinated globular macromolecules. The incorporation of iodine was also performed by postpolymerization chain-end modification to produce an X-ray opaque hyperbranched material.

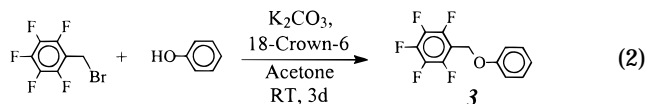
Results and Discussion

Synthesis. The monomer **1** used for the preparation of the hyperbranched polyfluorinated polymer **2** is an A₂B monomer, where A is the *p*-fluorine of the pentafluorophenyl functionality and B is the OH functionality. Reaction of 3,5-dihydroxybenzyl alcohol with α -bromopentafluorotoluene, in the presence of K₂CO₃ and 18-crown-6, in acetone at room temperature for 3 days gave **1** in 78% yield, after purification by silica flash chromatography. This monomer has been used



as a first-generation dendron in a multistep synthesis of pentafluorophenyl-terminated dendrimers,¹² where it was found that the *p*-fluorines of the pentafluorophenyl groups were selectively displaced by nucleophiles, thereby making the direct polymerization of **1** possible. This chemistry is similar to the nucleophilic aromatic substitution reactions used to prepare linear aryl fluoride poly(ether)s^{8g,13} and also employed by Miller and Neenan^{11b,c} in the preparation of hyperbranched poly(aryl ether)s. However, our monomer contains a benzylic alcohol rather than a phenol, and we employ different reagents and significantly lower polymerization temperatures.

Polymerization of **1** requires deprotonation of the benzylic alcohol to increase its nucleophilicity and allow for attack upon the *p*-fluorine of the pentafluorophenyl rings. The agent used for deprotonation must selectively abstract the hydroxyl proton and also must be non-nucleophilic. To investigate the feasibility of various bases, α -phenoxy-pentafluorotoluene (**3**) was used as



a model compound. The preparation of **3** was by reaction of phenol with K₂CO₃ and α -bromopentafluorotoluene in acetone at room temperature for 3 days. Purification by silica flash chromatography gave **3** in 71% yield. A hydroxyl functionality is lacking in **3**, while the benzylic methylene and aryl protons are present for detection of unwanted proton-abstraction reactions. The pentafluorophenyl unit of **3** allows for the determination of unwanted nucleophilic displacement reactions by the base.

Several bases and reaction conditions were investigated. 1,4-Diazabicyclo[2.2.2]octane (DABCO), 2,2,6,6-tetramethylpiperidine (TMP), and proton sponge gave no reaction with **3** but also did not promote the polymerization of **1**. Pyridine, 1,8-diazabicyclo[5.4.0]undec-7-ene (DBU), and *N,N,N,N*-tetramethylethylenedi-

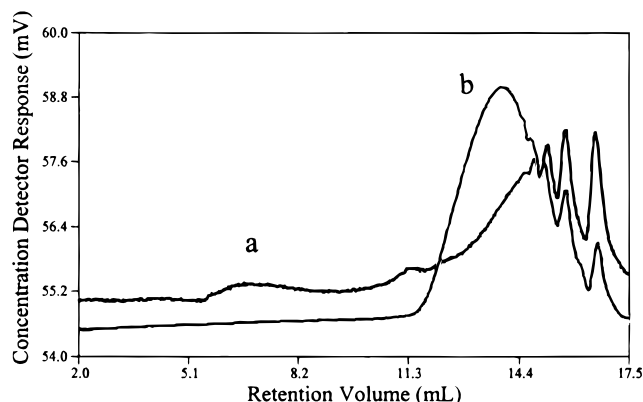


Figure 1. Gel permeation chromatography traces demonstrating the different molecular-weight distributions obtained using different sizes of sodium particles for the polymerization of **1**, where (a) is for sodium pieces with >1-mm diameter and (b) is for a sodium dispersion with sodium particle sizes <0.1 mm.

amine (TMEDA) resulted in unidentified polar products when reacted with **3** and with **1** at elevated temperatures, which may be due to attack upon the *p*-fluorine.¹⁴ Bases that caused polymerization of the model compound, **3**, include potassium bis(trimethylsilyl)amide (above -78°C), lithium diisopropylamide (LDA) (above -78°C), and *sec*-BuLi. This polymerization appeared to occur via deprotonation of the benzylic methylene protons followed by attack of the carbanion upon the pentafluorophenyl ring, as determined by a combination of ¹H and ¹⁹F NMR. The polymerization of **1** using potassium bis(trimethylsilyl)amide went cleanly at -78°C , but only when the base was fresh. Excess K₂CO₃ or Cs₂CO₃ in DMF at room temperature or in toluene at reflux gave no side reactions with **3** and were then found to afford polymerization of **1**; however, only low yields of **2** were isolable. Reaction of **1** with sodium hydride in THF at 50°C , followed by dimethyl sulfoxide (DMSO) at 100°C ,^{11b} gave decomposition to brown-colored insoluble products without observable polymerization.

Sodium metal was found to give no reaction with **3** and was then investigated for the polymerization of **1**. The surface area of the sodium was found to have an effect on the polymer molecular weight, the polymer yield, the molecular weight distribution, and the apparent rate of polymerization. The use of small sodium pieces (<0.1 mm, suspension in toluene) led to high yields of low-molecular-weight products and almost no monomer remaining. In contrast, the use of large sodium pieces (>1 mm) led to low yields of high-molecular-weight polymers and large amounts of monomer and oligomers remaining (Figure 1). Reproducible results were achieved with sodium that was <0.1 mm in size (30 wt % suspension in toluene).

The effects of polymerization temperature (Figure 2) and monomer concentration (Figure 3) were evaluated by measurements of molecular weight versus time upon reaction of **1** with sodium. Three different temperatures (room temperature, 40°C , and reflux) were used for the polymerizations of **1** at 0.3 M concentration in THF, and polymerizations were performed with three different concentrations of **1** (0.1, 0.3, and 0.5 M) in THF at 40°C . The molecular weights for this study were measured by gel permeation chromatography (GPC), in comparison to polystyrene standards. The results show that lower reaction concentrations and lower temperatures led to longer reaction times and lower molecular weight

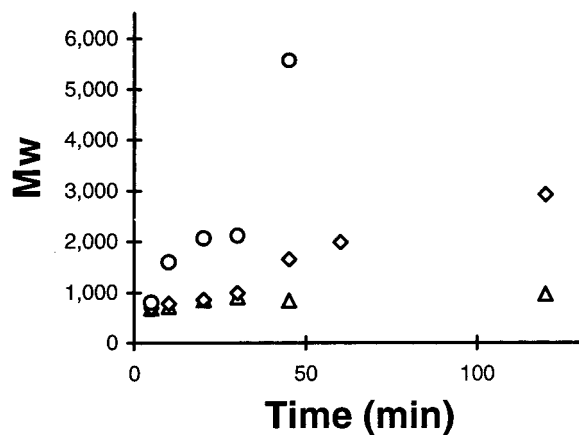


Figure 2. Dependence of the molecular weight of **2** with variation in polymerization temperature plotted as M_w versus time for polymerizations of **1** as 0.3 M solutions in THF with 1.5 equiv of sodium (<0.1 mm particle size, 30 wt % dispersion in toluene) at (Δ) 25 °C, (◇) 40 °C, and (○) reflux.

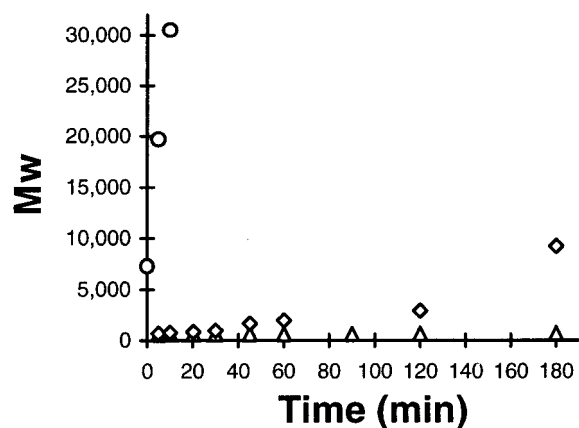


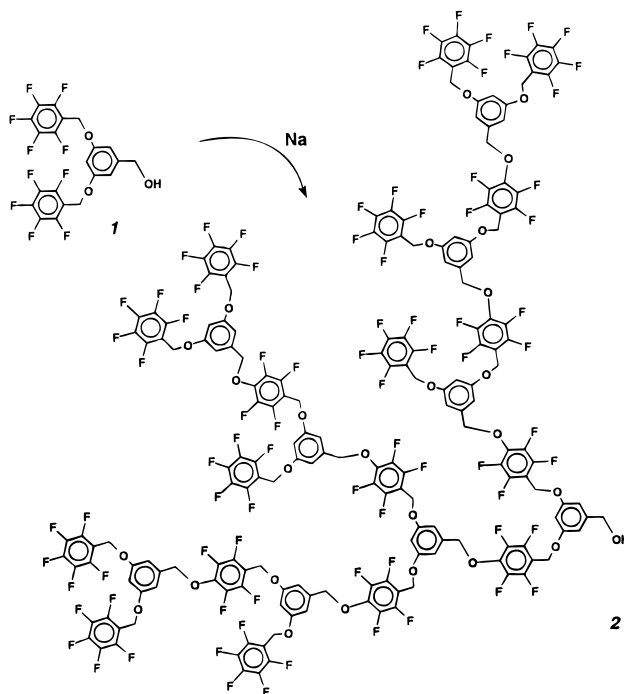
Figure 3. Effect of monomer (**1**) concentration upon the molecular weight of **2**, plotted as M_w versus time for polymerization of **1** in THF with 1.5 equiv of sodium (<0.1-mm particle size) at 40 °C and concentrations of (Δ) 0.1 M, (◇) 0.3 M, and (○) 0.5 M.

products. The combination of high concentrations of **1** and high temperatures gave precipitation during polymerization and some insoluble products (usually <10%).

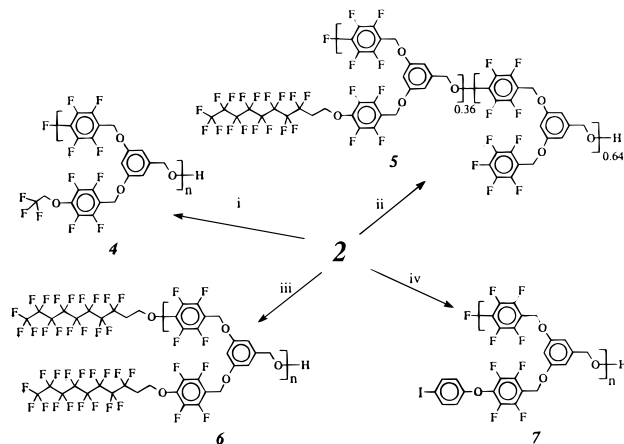
Optimum polymerization conditions involved the reaction of **1** at 0.4 M in THF heated at reflux in the presence of sodium (<0.1 mm, 30 wt % suspension in toluene) (Scheme 1). The polymerization was quenched by precipitation of **2** into water directly from the reaction mixture. Centrifugation allowed for the water to be decanted and for **2** to be collected. Silica flash chromatography with 30% hexanes/ CH_2Cl_2 as the eluent removed the high-molecular-weight polymer from the oligomers and the remaining monomer. Oligomers and remaining monomer could be reused for polymerization. Even the high-molecular-weight samples of **2** are soluble in common organic solvents, such as THF, DMF, CH_2Cl_2 , CHCl_3 , toluene, and acetone; however, as previously mentioned, insoluble products were also obtained in some cases.

Determination of the degree of branching was not possible, but it is expected that the polymerization occurs to yield the statistical 50% branching.¹⁵ The polymer **2** contains an overall average composition of one pentafluorophenyl group per each monomeric repeat unit plus one additional pentafluorophenyl end group,

Scheme 1. Synthesis of the Pentafluorophenyl-terminated Hyperbranched Benzyl Ether Polymer **2**



Scheme 2. Chemical Modification of **2**^a



- $\text{CF}_3\text{CH}_2\text{OH}$ (1.2 equiv.), *sec*-BuLi (1.0 equiv.), THF, 50 °C, 3d;
- $\text{CF}_3(\text{CF}_2)_7(\text{CH}_2)_2\text{OH}$ (1.5 equiv.), *sec*-BuLi (1.2 equiv.), THF, 50 °C, 3d;
- $\text{CF}_3(\text{CF}_2)_7(\text{CH}_2)_2\text{OH}$ (5.4 equiv.), *sec*-BuLi (4.9 equiv.), THF, 50 °C, 3d;
- p*-iodophenol (1.0 equiv.), K_2CO_3 , 18-C-6, DMF, 50 °C, 3d.

^a Only the overall compositional repeat units are shown, even though each of the polymers contains, a combination of linear, branched, and terminal units.

which were then used as reactive sites for modification of the physical and chemical properties. To increase the fluorocarbon character and decrease the reactivity of **2**, perfluoroalkyl chains were incorporated into the structure. This was accomplished by nucleophilic aromatic substitution of the *p*-fluorines by perfluoroalkoxy moieties (Scheme 2).

The 2,2,2-trifluoroethoxy-substituted hyperbranched polyfluorinated benzyl ether polymer **4** was synthesized by deprotonation of trifluoroethanol using *sec*-butyllithium, followed by addition of the lithium trifluoroethoxide to **2** in THF and heating at 50 °C under argon for 3 days. When 1.5 equiv of 2,2,2-trifluoroethanol and 1.2 equiv of *sec*-butyllithium were used, 91% of the

p-fluorine chain ends were substituted, as determined by ^{19}F NMR. Purification by precipitation into water to remove excess 2,2,2-trifluoroethanol, followed by silica flash chromatography twice, gave **4** in 38% yield.

The 1*H*,1*H*,2*H*,2*H*-perfluorodecanoxy-substituted hyperbranched polyfluorinated benzyl ether polymers **5** and **6** were synthesized in the same manner as for **4**, with the exception that the alcohol used was 1*H*,1*H*,2*H*,2*H*-perfluorodecanol. A large excess of alcohol was needed to achieve high substitution: 1.2 equiv of lithium 1*H*,1*H*,2*H*,2*H*-perfluorodecanoxy yielded 36% substitution (**5**), while 4.9 equiv yielded 95–100% substitution (**6**). Purification of **5** and **6** was by repeated precipitation into hexane to remove excess alcohol and then by silica flash chromatography twice to yield 34% and 43%, respectively. The low yields obtained were due to isolation and purification difficulties.

To synthesize a polymer that is visible under X-ray, iodine was incorporated (**7**). The nucleophilic substitution of **2** with 2,4,6-triodophenol was attempted, but no reaction occurred.¹⁶ In contrast, reaction with *p*-iodophenol (Scheme 2) occurred under mild conditions. A mixture of **2** and *p*-iodophenol was allowed to react with K_2CO_3 and 18-crown-6 in THF at room temperature under argon for 3 days. Purification of **7** was by repeated silica flash chromatography using 70% hexanes/ CH_2Cl_2 as eluent and gradually increasing the polarity to CH_2Cl_2 . Due to difficulties in the separation of **7** from the remaining *p*-iodophenol, the yield of **7** was only 35%. The resulting polymer (**7**) contained *p*-iodophenyl tetrafluorophenyl ether groups at 90% of the chain ends, as determined by ^{19}F NMR, and was observable under X-rays.

Characterization. All of the compounds were characterized by standard techniques including infrared spectroscopy, ^1H , ^{13}C , and ^{19}F NMR spectroscopy, elemental analysis, gel permeation chromatography (GPC), and differential scanning calorimetry (DSC). ^{19}F -decoupled ^{13}C NMR was also used for **2**, **5**, and **6**.

Molecular weights were measured by GPC in comparison to polystyrene standards. The number-average molecular weights (M_n) of samples having lower degrees of polymerization were also calculated by ^1H and ^{19}F NMR analysis. The ^1H NMR end-group analysis involved comparison of the intensities of the resonance at 4.4 ppm, due to the benzyl alcohol methylene protons of the unique B focal point functionality, and the resonances from 4.5 to 5.0 ppm resulting from the other benzylic methylene protons within the polymer, in toluene-*d*₈ or CDCl_3 solvent. Calculation of the degree of polymerization (DP_n) by ^{19}F NMR relied upon the ratio of *p*-fluorines from pentafluorophenyl groups at -153.6 ppm versus *o*- or *m*-fluorines of the tetrafluorophenyl rings at -144.8 or -156.9 ppm, respectively, that result from polymer growth. In this case, $p/m = [\text{DP}_n + 1]/[2(\text{DP}_n - 1)]$, where p/m is the ratio of *p*-fluorines of the pentafluorophenyl groups to *m*-fluorines of the tetrafluorophenyl groups. As is shown in Table 1, the M_n values calculated by GPC with PS standards and by NMR agree well in the low-molecular-weight range, up to M_n values of approximately 5000, even though polystyrene is a nonfluorinated, linear material. At higher average degrees of polymerization, error in the NMR calculation renders this method useless. For higher molecular weight products, viscosity and light-scattering detection were useful for measuring M_w , especially since some of the samples contained

Table 1. Comparison of Molecular Weights Obtained by Different Methods for Two Oligomer (I, II) and Two Polymer (III, IV) Samples of **2^a**

sample	PS equiv		^1H NMR M_n^b	^{19}F NMR M_n^c	LALLS M_w^d	SEC3 M_w^e
	M_w	M_n				
I	1000	700	600	600		
II	1600	1000	800	1000		
III	above calibration	6000	4000	5000	311 000	376 000
IV	above calibration	123 000			1 054 000	1 477 000

^a The samples were obtained from different polymerization conditions: **I** from reaction of 0.1 M **1** in THF with sodium (<1 mm, 30 wt% suspension in toluene) at 40 °C for 1 h; **II** from reaction of 0.3 M **1** in THF with sodium (<1 mm, 30 wt% suspension in toluene) at 40 °C for 45 min; **III** from reaction of 0.5 M **1** in THF with sodium (1–5-mm-diameter pieces) 40 °C for 8 h; **IV** from reaction of 0.5 M **1** in THF with sodium (1–5-mm-diameter pieces) at 40 °C for 9 h. ^b End group analysis. ^c Degree of polymerization calculated from the *p*-fluorine of the pentafluorophenyl group and the *m*-fluorine of the tetrafluorophenyl group. ^d Low-angle laser light scattering. ^e Calculated from triple detection including refractive index, viscometry, and low-angle laser-light-scattering measurements.

fractions of material at shorter retention times than those for the highest PS standard of 2 000 000 Da. Both methods agreed well (Table 1). Hyperbranched polymers are generally considered to give inaccurately low molecular weight characterization by GPC analysis, based upon linear standards, due to the decreased volume imposed by branching. In the case of the hyperbranched polyfluorinated materials, the fluorocarbon content may result in lower retention volumes, while the branching increases the retention volumes. Thus, overall, the molecular weights would agree with the linear polystyrene standards. An alternative explanation would be that the degrees of branching for the polymers studied are low. The degrees of branching should be the statistical 50%, and we are currently investigating selective degradation mechanisms to experimentally determine the extent of branching. A fluorocarbon effect upon the GPC analysis is supported by the finding that, with substantial fluorocarbon content, **6** gave a GPC M_w of 33 000 when the theoretical M_w based upon functionalization of the starting polymer **2** ($M_w = 7900$) was 14 000 Da.

Differential scanning calorimetry (DSC) was used to characterize the thermal transitions. The monomer, **1**, displayed a T_g at 4 °C and a melting point at 98–100 °C. With increasing molecular weight, the melting transition disappeared and the glass transition temperature increased, reaching a $(T_g)_\infty$ at 54 °C for **2** having $M_w > 20$ 000 Da. Upon functionalization of **2** with perfluoroalkyl chains, the T_g decreased to 45 and 47 °C for **4** and **5**, respectively, while the T_g remained the same (54 °C) for **6**.

Thermogravimetric analysis (TGA) was used to measure the thermal stabilities of the samples. The polymers showed no mass loss up to 300 °C while the samples were run under nitrogen or air. For **2** under N_2 , 25% of the mass was lost from 310 to 370 °C, followed by a second step of decomposition from 370 to 500 °C, corresponding to 15% mass loss, and 60% of the material remained. Under air, the same two-step mass loss was observed with the first loss of 25% occurring from 305 to 360 °C, 15% mass loss from 360 to 475 °C, and 50% of the material remaining at 500 °C. The thermal behavior for **6** was similar to that of **2**, although a higher fraction of the sample decomposed to volatile

Table 2. Contact Angles Measured with the Sessile Drop Method,¹⁷ after 30 s and 4 min with Water and after 30 s with Hexadecane

	contact angle (deg)		
	water		hexadecane
	30 s	4 min	30 s
1	69 ± 1.7	30 ± 0.6	18 ± 2.0
2	96 ± 2.3	91 ± 2.2	21 ± 2.2
4	99 ± 1.1	95 ± 1.7	14 ± 1.1
5	120 ± 1.1	120 ± 1.6	62 ± 2.0
6	120 ± 1.8	120 ± 2.1	67 ± 3.0

species. Under N₂, the TGA trace for **6** consisted of a main loss of 43% of the mass from 310 to 410 °C, followed by gradual loss of 12% of the mass from 410 to 500 °C, with 45% of the material remaining. In air, 35% mass loss was observed from 310 to 375 °C, followed by 35% mass loss from 375 to 500 °C, and only 30% of the material remained.

The contact angles of water (θ_{water}) and hexadecane ($\theta_{\text{hexadecane}}$) were measured by the sessile drop method¹⁷ on the surfaces of films of **2** and its derivatives, **4**, **5**, and **6** (Table 2). The hydrophobicity of **1** was not high, $\theta_{\text{water}} = 69^\circ$, most likely due to the OH functionality. The large decrease in the contact angle of water upon **1** after 4 min suggests rearrangement of the molecules to present the OH functionality toward contact with the water drop. Upon polymerization of **1**, the concentration of OH groups decreased, and this was seen by increased hydrophobicity, in which the contact angle of water upon **2** was 96° . The addition of trifluoroethoxy groups (**4**) did not substantially change the hydrophobicity of the material. However, substitution of only 36% of the chain ends with 1*H*,1*H*,2*H*,2*H*-perfluorodecanoxy groups (**5**) increased the contact angle to $\theta_{\text{water}} = 120^\circ$. The contact angle of water on poly(tetrafluoroethylene) (PTFE) was 115° , under our conditions. Comparison of **2**, **5**, and **6** indicates that the contact angle did not change further when 100% of the *p*-fluorines were substituted with 1*H*,1*H*,2*H*,2*H*-perfluorodecanol (**6**).

Each of the materials **1**, **2**, and **4** was not very lipophobic, with $\theta_{\text{hexadecane}} = 18^\circ$, 21° , 14° , respectively. The highest lipophobicity was seen for **5** and **6**, and these contact angles ($\theta_{\text{hexadecane}} = 62^\circ$ and 67° , respectively) were considerably higher than the contact angle of PTFE ($\theta_{\text{hexadecane}} = 42^\circ$) under these conditions. The difference of lipophobicity between **5** and **6** was only 5° for a difference of 64% in substitution.

Atomic force microscopy (AFM) was used to study the morphology and surface properties of the materials. The morphology of films of **2**, **5**, and **6** (Figure 4) was studied in tapping mode.¹⁸ Surfaces of spin-coated films of **2** and **6** (Figure 4a and d) exhibited uniform fractal morphology, characteristic for glassy polymers¹⁹ with root-mean-square surface roughness in the range 0.17–0.26 nm (see also Table 3). Ultrathin films of **5**, in which only 36% of available sites were substituted with fluoroalkyl chains, exhibited markedly different morphology (Figure 4b) with distinct 4 ± 1 nm protrusions (average height based on bearing analysis). The lateral size of the protrusions did not exceed 100 nm. Such morphology suggests phase separation between the fractions with different extents of substitution. Phase separation appeared to be enhanced in a thick film of **5** prepared by slow evaporation of solvent (Figure 4c), with the lateral size of protrusions exceeding 1 μm . Phase separation might be due to the fluorophobic effect²⁰ or

to surface segregation⁸ of the perfluoroalkyl chains. Due to similar T_g 's for the substituted and unsubstituted polymers, this phase separation was not detected by DSC. The presence of such aggregates in bulk material is being further investigated by solid-state NMR experiments.

The surface properties of **2**, **5**, and **6** were studied with lateral force experiments using contact mode AFM.²¹ In contact mode AFM imaging, the probe is scanned in an *X*–*Y* raster manner with respect to the surface, while the feedback system adjusts the *Z* position of a sample to maintain the constant vertical deflection of a cantilever (constant external normal force, F_{ne}). The probe scanned across the surface experiences the lateral friction force F_f acting in the direction opposite to the scan direction and equal to

$$F_f = \mu F_n \quad (3)$$

where μ is the coefficient of friction and F_n is the total normal force, which is the sum of the constant external normal force F_{ne} and the adhesive force F_a between the probe tip and the sample surface. Under the influence of a friction force, F_f , the cantilever undergoes additional deformation, which, if the scan direction is perpendicular to the long axis of the cantilever, is manifested as torsional deflection

$$\Delta\Phi = \pm F_f/k_t \quad (4)$$

where k_t is the torsional deformation spring constant of the cantilever. According to commonly adopted convention, the sign in eq 4 is positive for a scan direction from left to right (trace) and negative for a scan in the opposite direction (retrace). The torsional deflection gives rise to a voltage signal in the lateral deflection channel of the detector, which depending on the scan direction is equal to

$$L_t = c_1 F_f/k_t + o_{\text{ff}} \quad (5a)$$

or

$$L_r = -c_1 F_f/k_t + o_{\text{ff}} \quad (5b)$$

where the subscripts t and r correspond respectively to trace and retrace scan directions, o_{ff} is the signal offset depending on the laser beam alignment,²² and c_1 is the calibration coefficient for a lateral deflection signal. The offset and the differences in sign are eliminated in the difference lateral deflection signal L_s

$$L_s = (L_t - L_r)/2 = c_1 F_f/k_t \quad (6)$$

Combining eqs 1–4 yields

$$L_s = (c_1/k_t)\mu(F_{\text{ne}} + F_a) \quad (7)$$

Equation 7 predicts a linear dependence of L_s as a function of the external normal force F_{ne} with the slope proportional to the coefficient of friction μ and the *x*-intercept equal to the value of the adhesive force F_a . Determination of μ and F_a requires measurements at several different values of F_{ne} . To minimize the influence of changes of the probe tip upon prolonged scanning and to economize the measurements, we have developed a procedure in which F_{ne} is varied within a single run over a square area of a sample, as illustrated in Figure

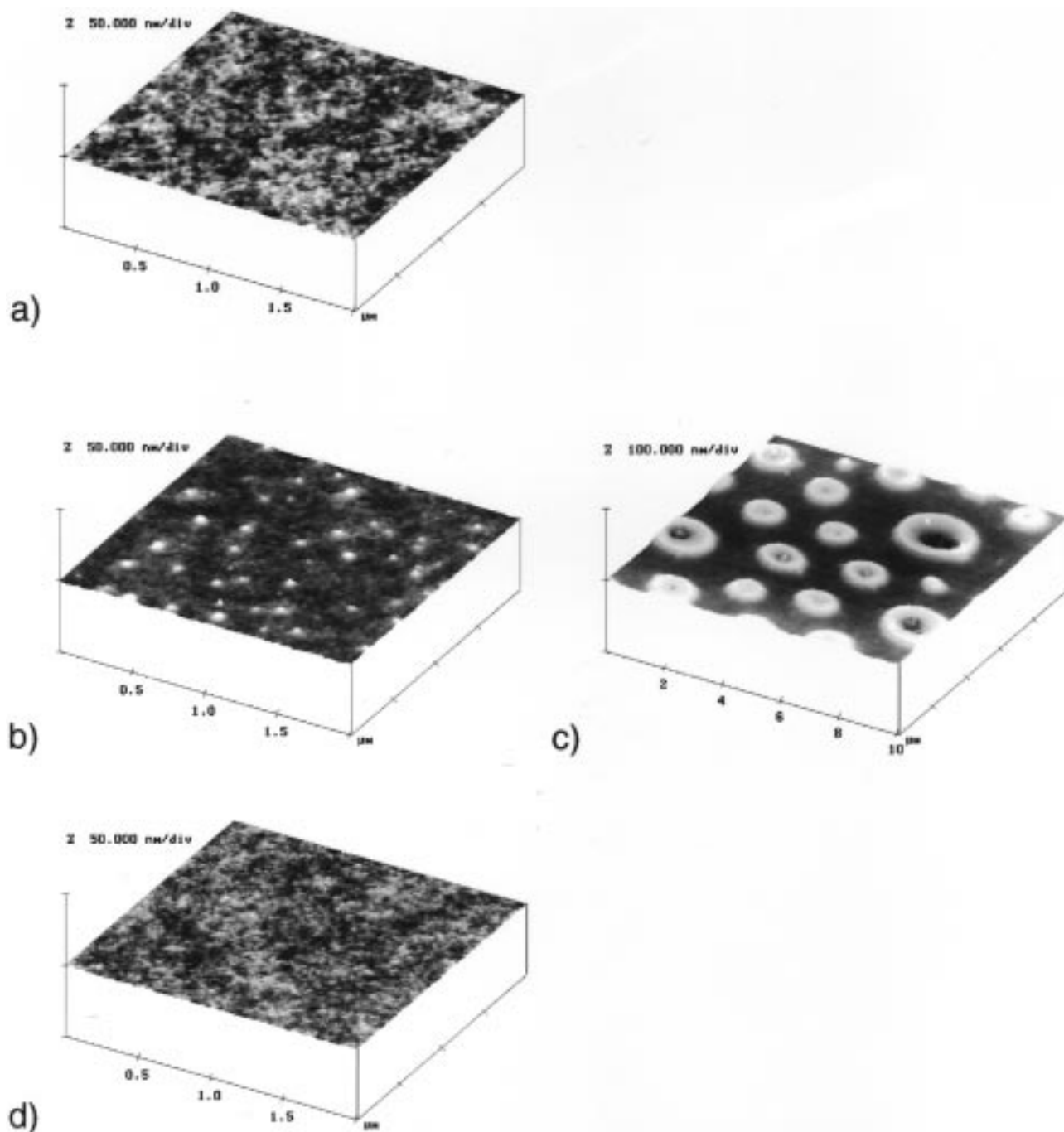


Figure 4. Tapping mode AFM topographs of surfaces of hyperbranched polyfluorinated polymers with different contents of long linear fluoroalkyl chains (see Schemes 1 and 2): (a, b, and d) ultrathin films of compounds **2**, **5**, and **6**, respectively, spin-coated on mica, scan size $2\ \mu\text{m} \times 2\ \mu\text{m}$, vertical scale 50 nm; (c) thick film of compound **5**, scan size $10\ \mu\text{m} \times 10\ \mu\text{m}$, vertical scale 100 nm. All images are presented in gray scale three-dimensional renderings with the color changing with height from black (lowest features) to white (tallest features).

5 (data for a Si_3N_4 tip on the surface of a silicon wafer). This procedure was applied to films of **2**, **5**, and **6** and, for comparison, to two common linear polymers—atactic polystyrene (*a*-PS, ultrathin film spin-coated on mica) and poly(tetrafluoroethylene) (PTFE, ultrathin film sputter-deposited on a silicon wafer). The external normal force F_{ne} was varied in 15-nN intervals from the value $F_{\text{ne}} = 0 \pm 2\ \text{nN}$ to $F_{\text{ne}} = 105\ \text{nN}$ (just below the threshold above which irreversible damage was observed).

In the current study, which had mostly comparative character, no attempt has been made to directly measure either the cantilever spring constants k and k_1 or

a calibration coefficient for torsional deflection of the cantilever, c_t . A nominal value of a spring constant, $k = 0.58\ \text{N/m}$,²³ was used in the calculations. To ensure direct comparability, the data for all materials were recorded with the same probe. The slopes of L_s versus F_{ne} were converted into the coefficient of friction values using relative calibration measurements on a surface of a silicon wafer as reference and using the value of $\mu = 0.06$, as determined by other authors for Si_3N_4 on silicon.²² To minimize the variability of results due to changes of the probe tip upon prolonged scanning, calibration runs were performed between each series of runs on a polymer film and the average value of relative

Table 3. Comparison of Surface Properties of Hyperbranched Polyfluorinated Polymers and Two Common Linear Polymers Determined by Atomic Force Microscopy

compound	sample	mole % F	weight % F	rms roughness ^a (nm)	coefficient of friction ^b μ ($\times 10^{-2}$)	adhesive force F_a ^c (nN)
2	ultrathin film surface	21.4	35.6	0.21 ± 0.04	6.5 ± 0.8	93 ± 7
5	ultrathin film surface	24.5 ^d	45.0 ^d	0.23 ± 0.03	4.2 ± 0.4	39 ± 1
	ultrathin film elevated domains				5.5 ± 1.2	38 ± 12
	thick film surface				3.5 ± 0.7	43 ± 7
	thick film elevated domains				6.8 ± 0.7	38 ± 3
6	ultrathin film surface	30.1	52.3	0.24 ± 0.02	2.8 ± 0.3	38 ± 8
a-PS	ultrathin film surface			0.22 ± 0.01	6.8 ± 0.4	57 ± 2
PTFE	ultrathin film surface	66.7	76.0	0.33 ± 0.01	4.7 ± 0.4	57 ± 4

^a Determined from tapping mode of AFM topographs obtained in $2 \mu\text{m} \times 2 \mu\text{m}$ scans with standard silicon probe. ^b Based on LFM measurements with standard Si_3N_4 tip, calibrated against native oxide on Si monocrystal, assuming the value of the coefficient of friction to be 0.006.²² ^c Calculated as an x -intercept from LFM friction measurements with a standard $120\text{-}\mu\text{m}$, wide-legged Si_3N_4 cantilever, using the nominal cantilever spring constant value equal to 0.58 N/m , as specified by the manufacturer.²³ ^d Overall composition.

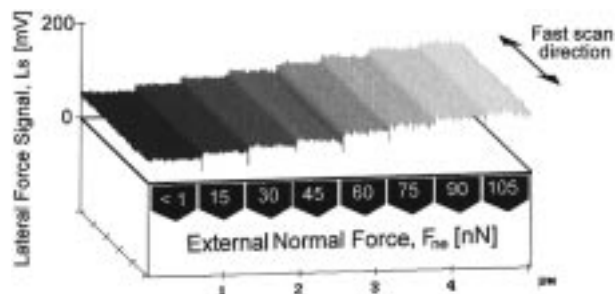


Figure 5. Typical results of a single-run friction experiment obtained with a Si_3N_4 tip on a native oxide surface of a Si monocrystal. In this experiment the tip was scanned in a $5 \mu\text{m} \times 5 \mu\text{m}$ square with a frequency of 2.93 lines/s and the fast scan direction perpendicular to the long axis of a cantilever. The external normal force F_{ne} was increased in a stepwise manner in eight equal time intervals, by incrementing the set point by a constant value. The plotted data correspond to a difference lateral force signal $L_s = (L_t - L_r)/2$, where L_t and L_r denote signals recorded in opposite scan directions (trace and retrace, respectively).

calibration coefficients measured before and after each series was used in each calculation.

Results for **2**, **5**, and **6** are shown in Figure 6 as plots of the average values of L_s within rectangular areas corresponding to the same value of external normal force, and AFM surface characterization data for all polymers are summarized in Table 3. The linear dependence of L_s versus F_{ne} predicted by eq 7 was confirmed in all studied cases in the force range up to $F_{ne} = 105 \text{ nN}$. The values of F_a determined from extrapolated x -intercepts of L_s versus F_{ne} were in good agreement with the maximum values of an adhesive force determined from force curve experiments.²⁴ The relative error of the coefficients of friction derived from the slopes was typically about $\pm 10\%$ (see Table 3), due to compounding of the error in determination of relative calibration coefficients before and after each series. Errors due to location on the surface, tip wear, and sample thickness were not significant, as observed by the differences in slopes of L_s versus F_{ne} measured in consecutive runs in different areas of the samples.

Data presented in Figure 6 and Table 3 clearly demonstrate more than a 2-fold decrease of the coefficient of friction μ and of the adhesive force F_a upon substitution with fluoroalkyl chains onto a hyperbranched polymer (**2** vs **6**). Films of **5** (partially substituted) exhibited mixed characteristics depending on the region of the film. Since the surface roughnesses of all films, as determined from tapping mode AFM topographs, were similar (Table 3), all observed differ-

ences should be ascribed to differences in chemical composition of the surfaces. Comparison of the coefficients of friction for **2**, **5**, and **6** suggests that the phase-separated domains in **5** are composed of mainly the parent pentafluorophenyl-terminated polymer, while the areas between the phase-separated domains contain the fluoroalkyl-chain-substituted polymer. The results obtained for **2** and a-PS (Table 3) indicate that fluorination of phenyl rings alone is not sufficient for lowering the coefficient of friction and decreasing the adhesive character of the surface. On the other hand, it is worth noting that the coefficient of friction μ and the adhesive force F_a , observed for **6** were significantly lower in comparison with those of PTFE, despite substantially higher fluorine content for PTFE. We propose that this points to a very high effectiveness of substitution with relatively short fluoroalkyl chains in modification of surface properties. Such effectiveness may stem from a large fraction of chain-end CF_3 groups introduced into the material and from high molecular mobility of the fluoroalkyl chains.

Experimental Section

Measurements. IR spectra were obtained on a Mattson Polaris spectrometer as thin films on NaCl disks. ^1H NMR spectra were recorded on solutions in CDCl_3 or toluene- d_8 on a Varian Unity 300 MHz spectrometer with the solvent proton signal as standard. ^{13}C NMR spectra were recorded at 75.4 MHz on solutions in CDCl_3 or toluene- d_8 on either a Varian Unity 300 spectrometer or a Varian 500 spectrometer with the solvent carbon signal as standard. ^{19}F NMR spectra were recorded at 282.2 MHz on solutions in CDCl_3 or toluene- d_8 on a Varian Unity 300 spectrometer with external CFCl_3 as standard.

Gel permeation chromatography (GPC) was conducted on a Hewlett-Packard series 1050 HPLC with a Viscotek model 110 differential viscometer, a Wyatt MiniDawn low-angle laser-light-scattering (LALLS) detector, and a Hewlett-Packard 1047A refractive index detector connected in series: data analysis was done by Viscotek (Houston, TX) Trisec GPC Software, v. 2.70, and Trisec GPC-LS-Viscometry (SEC³) software v. 3.0. Two $5\text{-}\mu\text{m}$ Polymer Laboratories PL gel columns ($300 \text{ mm} \times 7.7 \text{ mm}$) connected in series in order of increasing pore size (500 \AA , mixed bed C) were used with THF distilled from CaH_2 as solvent.

Glass transition temperatures (T_g s) were measured by differential scanning calorimetry (DSC) on a Perkin-Elmer DSC-4 differential scanning calorimeter. Heating rates were $10 \text{ }^\circ\text{C/min}$, and the T_g was taken as the midpoint of the inflection tangent, upon the third or subsequent heating scan. Thermogravimetric analyses (TGAs) were done on a Perkin-Elmer TGS-2 thermogravimetric analyzer. For both DSC and TGA, the Perkin-Elmer instruments were upgraded with Instrument Specialists, Inc. (Antioch, IL) temperature program

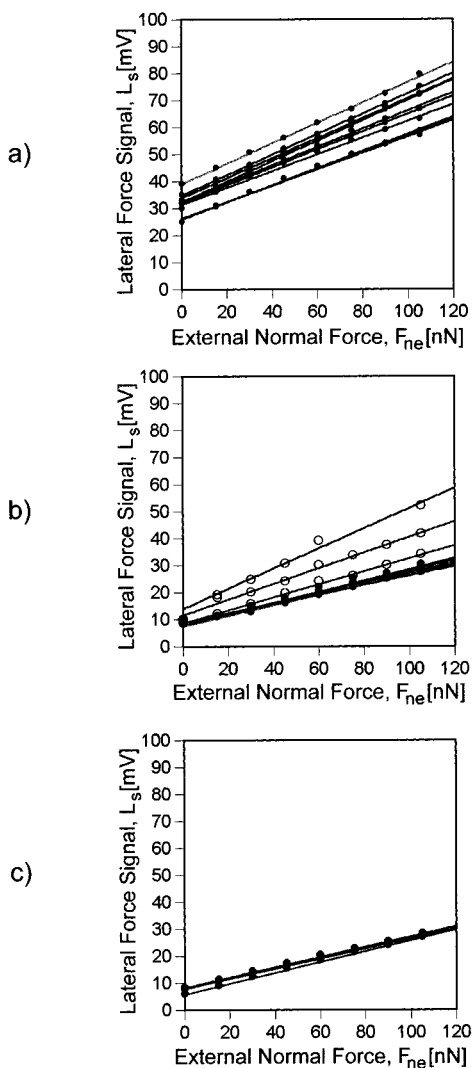


Figure 6. Lateral force signal L_s as a function of external normal force F_{ne} recorded with a Si_3N_4 tip on the surfaces of hyperbranched polyfluorinated polymers with different contents of long linear fluoroalkyl chains (see Schemes 1 and 2): (a) **2**; (b) **5**, solid circles—between phase-separated regions, open circles—in phase-separated regions (see Figure 4b and c); (c) **6**. Data points are the average values measured in rectangular areas corresponding to the same value of normal force (see Figure 6); lines represent linear least-squares fits. The slope of L_s versus F_{ne} is directly proportional to the coefficient of friction; the extrapolated x -intercept is equal to the adhesive force F_a (see eq 7). All the data were acquired in one series with the same cantilever, in an atmosphere of helium at room temperature. Data presented in (b) and (c) were acquired on ultrathin, spin-coated films of polymers in a series of consecutive runs in different locations on the sample surface. To illustrate the extent of scatter due to tip wear upon prolonged scanning and due to different sample preparations, the data presented for **2** are the combined results of experiments performed on ultrathin and thick films and at the beginning and at the end of an entire series of measurements for ultrathin films.

interface-PE, and data were acquired and analyzed using TA-PC software version v. 2.11 (Instrument Specialists, Inc.).

Contact angles were measured as static contact angles with the sessile drop technique¹⁷ using a TanteC CAM-micro contact angle meter and the half-angle measuring method. The samples were prepared by solution casting of the materials as two to three layers from 0.05 M CH_2Cl_2 solutions onto a microscope slide to produce films of approximately 0.5- μm thickness, which were allowed to dry for at least 2 h. Contact angles of water (4 μL) were measured on the films 30 s and 4

min after drop application, contact angles of hexadecane (4 μL) were only measured after 30 s, and an average of five measurements are given.

Atomic force microscopy studies of micromechanical properties of ultrathin films of hyperbranched polymers were carried out with the aid of a Nanoscope III-M system (Digital Instruments, Santa Barbara, CA), equipped with the J-type vertical engage scanner. Contact mode experiments were performed with standard, 100 μm -long, wide-leg Si_3N_4 cantilevers (nominal spring constant 0.58 N/m). Tapping mode imaging was carried out with silicon cantilevers (typical resonance frequency ca. 300 MHz, nominal spring constant ca. 50 N/m, length 120 μm). Tapping mode images were acquired in 2 $\mu\text{m} \times 2 \mu\text{m}$ (512 points \times 512 points) scans (scan rate 2.93 lines/s) with cantilever oscillation signals between 0.2 and 0.3 V, at set points corresponding to 95% of the "free" oscillation amplitude. All experiments were performed under an atmosphere of dry He to ensure uniform conditions, independent of ambient atmosphere, in particular to minimize the role of humidity. Freshly cleaved mica (New York Mica Company) was used as a substrate for ultrathin films, which were spin-coated by directly depositing a 7 μL drop of solution of hyperbranched polymers in CHCl_3 (typical concentration range 2–5 mg/mL) at the surface of substrates rotating at 4000 rpm. The film thicknesses were measured with AFM by measuring the depths of 1 $\mu\text{m} \times 1 \mu\text{m}$ holes machined with the probe operating at high contact force and were in the range 10–15 nm. Prior to AFM runs the films were dried under the rotary-pump vacuum in order to remove the solvent residues.

Materials. 1,1,1,3,3,3-Hexamethyldisilazane (HMDS, 98%), trimethylsilyl chloride (TMSCl, 98%), benzoyl peroxide (97%), potassium carbonate (99+%), 18-crown-6 (99%), phenol (99+%), sodium lump in kerosene (99%), 3,5-dihydroxybenzyl alcohol (99%), and potassium bis(trimethylsilyl)amide (95%) were purchased from Aldrich Chemical Co., Inc., and used as received. THF was distilled from sodium benzophenone, and DMF was distilled from CaO at 20 mmHg. *sec*-Butyllithium (1.3 M in cyclohexane/hexane (92/8)) and sodium (30 wt % dispersion in toluene, <0.1-mm particle size) were purchased from Acros Organics and were used as received. Pentafluorobenzyl bromide (97%), 2,2,2-trifluoroethanol (99+%), and 1*H*,1*H*,2*H*,2*H*-perfluorodecanol (97+%) were each purchased from PCR, Inc., and were used as received. Flash chromatography was performed using silica gel 60, 230–400 mesh (40–63 μm) from Mallinckrodt Chemical Company. Elemental analysis was performed by M-H-W Laboratories in Phoenix, Arizona.

3,5-Bis[(pentafluorobenzyl)oxy]benzyl Alcohol (1). A mixture of pentafluorobenzyl bromide (99.32 g, 380.6 mmol, 2.1 equiv) and 3,5-dihydroxybenzyl alcohol (25.57 g, 182.5 mmol, 1.0 equiv) was allowed to react with K_2CO_3 (52.88 g, 383.2 mmol, 2.1 equiv) in the presence of 18-crown-6 (ca. 0.1 equiv) in acetone (1 L) at RT, with vigorous mechanical stirring under Ar. After 3 days, the solvent was removed in vacuo, the residue was partitioned between water (300 mL) and CH_2Cl_2 (300 mL), the aqueous layer was extracted with CH_2Cl_2 (3 \times 200 mL), and the CH_2Cl_2 extracts were combined, dried over MgSO_4 , and concentrated in vacuo. A portion of the product, **1**, was obtained by crystallization from 50% hexane/ CH_2Cl_2 , with the remainder of the material being purified by flash chromatography eluting with 50% hexane/ CH_2Cl_2 , increasing polarity to CH_2Cl_2 : yield 71.10 g (78%); T_g 4 $^\circ\text{C}$; T_m 98–100 $^\circ\text{C}$; IR 3600–3100, 3100–2850, 1659, 1598, 1525, 1509, 1459, 1434, 1383, 1312, 1290, 1165, 1132, 1060, 977, 941, 830, 770, 685 cm^{-1} ; ^1H NMR (CDCl_3) δ 1.96 (t, 1H, $J = 6$ Hz, OH), 4.64 (d, 2H, $J = 6$ Hz, ArCH₂OH), 5.10 (s, 4H, C₆F₅CH₂O), 6.48 (t, 1H, $J = 2$ Hz, ArH), 6.65 (d, 2H, $J = 2$ Hz, ArH) ppm; ^{13}C NMR (CDCl_3) δ 57.5 (C₆F₅CH₂O), 64.9 (ArCH₂OH), 101.3, 106.3 (ArCH), 109.9 (m, pentafluorophenyl *ipso*-C), 137.6 (d of m, $^1J_{\text{C-F}} = 249$ Hz, C-F), 141.8 (d of m, $^1J_{\text{C-F}} = 256$ Hz, C-F), 144.0 (Ar *ipso*-C), 145.7 (d of m, $^1J_{\text{C-F}} = 249$ Hz, C-F), 159.4 (Ar *ipso*-C) ppm; ^{19}F NMR (CDCl_3) δ -143.0 (m, 4F, *ortho*-F), -153.3 (m, 2F, *para*-F), -162.3 (m, 4F, *meta*-F) ppm. Anal. Calcd for C₂₁H₁₀F₁₀O₃ (500.29): C, 50.42; H, 2.02; F, 37.98. Found: C, 50.49; H, 2.12; F, 38.21.

Synthesis of Hyperbranched Polyfluorinated Poly-(benzyl ether)s (2). To a 0.4 M solution of **1** (1.00 g, 2.00 mmol) in dry THF (4.8 mL) at room temperature under Ar was added sodium (0.17 mL, 2.0 mmol, 1.0 equiv) via syringe. Additional aliquots of sodium were added after 1 and 2 days. The reaction mixture was heated at reflux for a total of 3 days and allowed to cool to room temperature, and then the reaction was quenched by precipitation of the polymer into water. The product was isolated by centrifugation and further purified by flash chromatography eluting with 30% hexanes/CH₂Cl₂, increasing polarity to CH₂Cl₂, to give **2** as a transparent glass: yield 0.73 g (76%); $M_w = 9000$, $M_w/M_n = 2.2$, from GPC based upon PS standards; T_g 52 °C; IR 3100–2900, 1719, 1658, 1599, 1524, 1510, 1502, 1461, 1431, 1379, 1312, 1292, 1164, 1059, 1005, 977, 830, 770, 685 cm⁻¹; ¹H NMR (toluene-*d*₆) δ 4.5–4.8 (br m, 4 H, C₆F₄CH₂O and C₆F₅CH₂O), 4.8–5.0 (br s, 2 H, ArCH₂O), 6.5 (br m, 1 H, ArH), 6.7 (br m, ArH) ppm; ¹³C NMR (toluene): δ 57.3 (C₆F₄CH₂O), 57.6 (C₆F₅CH₂O), 75.9 (ArCH₂O), 102.5, 107.5 (ArCH), 109.3 (m, pentafluorophenyl *ipso*-C), 110.1 (m, tetrafluorophenyl *ipso*-CCH₂O), 137.4 (d of m, $J = 250$ Hz, ArCF), 137.8 (tetrafluorophenyl *ipso*-COCH₂O), 139.1 (m, Ar *ipso*-C), 141.9 (d of m, $J = 250$ Hz, ArCF), 145.9 (d of m, $J = 250$ Hz, ArCF), 146.3 (d of m, $J = 250$ Hz, ArCF), 160.0 and 160.1 (Ar *ipso*-C) ppm, assignments confirmed by ¹⁹F-decoupled ¹³C NMR at 125 MHz; ¹⁹F NMR (CDCl₃) δ -143.6 (m, 2F, pentafluorophenyl *ortho*-F), -144.8 (m, 2F, tetrafluorophenyl *ortho*-F), -153.59 (m, 1F, *para*-F), -156.94 (m, 2F, tetrafluorophenyl *meta*-F), -162.62 (m, 2F, pentafluorophenyl *meta*-F). Anal. Calcd for repeat unit C₂₁H₉F₉O₃ (480.28): C, 52.52; H, 1.89; F, 35.60. Found: C, 52.71; H, 2.01; F, 35.44.

α-Phenoxy-pentafluorotoluene (3). A mixture of α-bromopentafluorotoluene (5.01 g, 19.2 mmol) and phenol (1.81 g, 19.2 mmol) was allowed to react with K₂CO₃ (2.76 g, 20.0 mmol) in the presence of 18-crown-6 (0.49 g, 1.8 mmol) in acetone (50 mL) with vigorous stirring at room temperature under Ar. After 3 days, the solvent was removed in vacuo, the residue was partitioned between water (100 mL) and CH₂Cl₂ (100 mL), the aqueous layer was extracted with CH₂Cl₂ (3 × 50 mL), and the CH₂Cl₂ extracts were combined, dried over MgSO₄, and concentrated in vacuo. Purification by flash chromatography eluting with 80% hexane/CH₂Cl₂ gave **3** as a white solid: yield 3.74 g (71%); T_m 76.0–76.5 °C; IR 3100–2900, 1712, 1600, 1590, 1504, 1245, 1065, 1036, 941, 750 cm⁻¹; ¹H NMR (CDCl₃) δ 5.13 (s, 2H, C₆F₅CH₂O), 6.98 (d, 2H, $J = 8$ Hz, *ortho*-ArH), 7.03 (t, 1H, $J = 8$ Hz, *para*-ArH), 7.33 (overlapping dd, 2H, $J = 8$ Hz, *meta*-ArH) ppm; ¹³C NMR (CDCl₃) δ 57.4 (C₆F₅CH₂O), 110.3 (t, $J = 75$ Hz, pentafluorophenyl *ipso*-C), 114.8, 121.9, 129.6 (ArCH), 137.6 (d of m, $J_{C-F} = 249$ Hz, CF), 141.7 (d of m, $J_{C-F} = 256$ Hz, CF), 145.8 (d of m, $J_{C-F} = 249$ Hz, CF), 157.9 (Ar *ipso*-C); ¹⁹F NMR (CDCl₃) δ -143.4 (m, 4F, *ortho*-F), -154.4 (m, 2F, *para*-F), -163.2 (m, 4F, *meta*-F). Anal. Calcd for C₁₃H₇F₅O (274.19): C, 56.95; H, 2.57; F, 34.65. Found: C, 57.10; H, 2.65; F, 34.22.

2,2,2-Trifluoroethanoxy-Substituted 2 (4). To a solution of 2,2,2-trifluoroethanol (0.094 g, 0.94 mmol, 1.5 equiv) in THF (2 mL) at -78 °C was added *sec*-butyllithium (0.57 mL, 1.0 equiv) via syringe. The reaction mixture became clear and colorless and was allowed to warm to room temperature. This solution of the alkoxide was then added via syringe to a solution of **2** (0.30 g, 0.62 mmol of pentafluorophenyl functionalities, $M_w = 11\,000$, $M_w/M_n = 3.7$, from GPC based upon PS standards) in THF (2 mL) to make a 0.1 M solution, which was then heated at 50 °C under Ar for 3 days. The reaction was quenched by precipitation into water (500 mL). The polymer was isolated, redissolved into CH₂Cl₂, and purified twice by silica flash chromatography using 50% hexanes/CH₂Cl₂ as eluent to give **4**, containing 91% substitution of the *p*-fluorines in the ¹⁹F NMR, as a transparent glass: yield 0.13 g (38%); $M_w = 16\,000$, $M_w/M_n = 2.3$, from GPC based upon PS standards; $T_g = 45$ °C; IR 3100–2900, 1719, 1657, 1599, 1502, 1459, 1430, 1379, 1300, 1274, 1167, 1057, 1004, 976, 940, 835, 740, 703 cm⁻¹; ¹H NMR (CDCl₃) δ 4.4–4.6 (br s, 2 H, CF₃CH₂O), 5.0–5.2 (br s, 4 H, C₆F₄CH₂O), 5.2–5.4 (br s, 2 H, ArCH₂O), 6.5–6.6 (br m, 1 H, ArH), 6.6–6.8 (br m, 2 H, ArH)

ppm; ¹³C NMR (CDCl₃) δ 57.7 (C₆F₄CH₂O), 70.5 (m, CF₃CH₂O), 75.9 (ArCH₂O), 102.5 (ArCH), 107.5 (ArCH), 108.6 (m, tetrafluorophenyl *ipso*-C), 109.3 (m, tetrafluorophenyl *ipso*-C), 110.1 (m, tetrafluorophenyl *ipso*-C), 122.7 (m, CF₃), 136.7 (tetrafluorophenyl *ipso*-C), 137.3 (d of m, $J_{C-F} = 250$ Hz, ArCF), 137.8 (tetrafluorophenyl *ipso*-C), 138.4 (Ar *ipso*-C), 140.8 (d of m, $J_{C-F} = 250$ Hz, ArCF), 141.2 (d of m, $J_{C-F} = 250$ Hz, ArCF), 141.3 (d of m, $J_{C-F} = 250$ Hz, ArCF), 145.9 (d of m, $J_{C-F} = 250$ Hz, ArCF), 159.5 and 159.6 (Ar *ipso*-C) ppm, assignments confirmed by ¹⁹F-decoupled ¹³C NMR at 125 MHz; ¹⁹F NMR (CDCl₃) δ -75.4 (s, 3 F, CF₃), -142.7 (m, 2 F (9%), *ortho*-F), -143.3 (m, 2 F, ArF), -144.5 (m, 2 F, ArF), -152.7 (m, 1 F (9%), *para*-F), -156.5 (m, 2 F, ArF), -156.7 (m, 2 F, ArF), -161.8 (m, 2 F (9%), *meta*-F) ppm. Anal. Calcd for repeat unit 77% C₂₃H₁₁F₁₁O₄ (544.32), repeat unit 23% C₂₁H₉F₉O₃ (480.28): C, 50.04; H, 1.96; F, 36.91. Found: C, 51.41; H, 2.22; F, 37.51.

1H, 1H, 2H, 2H-Perfluorodecanoxy-Substituted 2 (5). This was prepared from 1H,1H,2H,2H-perfluorodecanol (0.42 g, 0.94 mmol, 1.5 equiv), *sec*-butyllithium (0.57 mL, 0.74 mmol, 1.2 equiv), and **2** (0.30 g, 0.62 mmol of pentafluorophenyl functionalities, 1.0 equiv, $M_w = 11\,000$, $M_w/M_n = 3.7$, from GPC based upon PS standards) by the same procedure as for the preparation of **4**. The product was purified twice by silica flash chromatography using 80% hexane/acetone to give **5** as a colorless glass, with 36% of the chain ends substituted by the perfluorodecanoxy group and 64% remaining as pentafluorophenyl groups, by ¹⁹F NMR: yield 0.089 g (34%); $M_w = 14\,000$, $M_w/M_n = 1.7$, from GPC based upon PS standards; $T_g = 47$ °C; IR 3100–2900, 1656, 1599, 1500, 1467, 1378, 1291, 1242, 1214, 1153, 1057, 1006, 941, 828, 730, 692 cm⁻¹; ¹H NMR (CDCl₃) δ 2.65 (br m, 2H (36%), CF₃(CF₂)₇CH₂CH₂O), 4.53 (br m, 2H (36%), CF₃(CF₂)₇CH₂CH₂O), 5.05 (br s, 4H, C₆F₄CH₂O), 5.19 (br s, 2H, ArCH₂O), 6.53 (br m, 1H, ArH), 6.70 (br m, 2H, ArH) ppm; ¹³C NMR (CDCl₃) δ 31.9 (t, $J = 17$ Hz, aliphatic CF₂CH₂), 57.6 (C₆F₄CH₂O), 57.7 (C₆F₄CH₂O), 66.8 (aliphatic CH₂O), 75.9 (ArCH₂O), 102.5 (ArCH), 107.3 (ArCH), 108.6 (m, tetrafluorophenyl *ipso*-C), 109.4 (m, CF₃), 109.5 (m, pentafluorophenyl *ipso*-C), 109.9 (m, tetrafluorophenyl *ipso*-C), 110.3 (m, aliphatic CF₂), 110.9 (m, aliphatic CF₂), 111.5 (m, aliphatic CF₂), 117.3 (m, aliphatic CF₂), 136.3 (d of m, $J = 250$ Hz, ArCF), 136.5 (m, tetrafluorophenyl *ipso*-C), 137.6 (m, tetrafluorophenyl *ipso*-C), 138.4 (Ar *ipso*-C), 140.9 (d of m, $J = 250$ Hz, ArCF), 141.2 (d of m, $J = 250$ Hz, ArCF), 142.0 (d of m, $J = 250$ Hz, ArCF), 145.8 (d of m, $J = 250$ Hz, ArCF), 159.3 (Ar *ipso*-C), 159.5 (Ar *ipso*-C) ppm; ¹⁹F NMR (CDCl₃) δ -81.3 (s, 3F (36%), aliphatic CF₃), -113.8 (s, 2F (36%), aliphatic CF₂), -122.4 (s, 6F (36%), aliphatic CF₂), -123.2 (s, 2F (36%), aliphatic CF₂), -124.0 (s, 2F (36%), aliphatic CF₂), -126.6 (s, 2F (36%), aliphatic CF₂), -142.8 (m, 2F (64%), C₆F₅ *ortho*-F), -144.1 (m, 2F (36%), C₆F₄ArF), -144.4 (m, 2F, C₆F₄ArF), -153.0 (m, 1F (64%), C₆F₅ *para*-F), -156.5 (m, 2F, C₆F₄ArF), -157.2 (m, 2F (36%), C₆F₄ArF), -162.0 (m, 2F (64%), C₆F₅ *meta*-F) ppm. Anal. Calcd for 36% repeat unit of C₃₁H₁₃F₂₅O₄ (924.40), 64% repeat unit of C₂₁H₉F₉O₃ (480.28): F, 44.97. Found: F, 42.52.

1H, 1H, 2H, 2H-Perfluorodecanoxy-Substituted 2 (6). This was prepared from 1H,1H,2H,2H-perfluorodecanol (9.27 g, 20.8 mmol, 5.4 equiv), *sec*-butyllithium (17.2 mL, 18.7 mmol, 4.9 equiv) and **2** (1.85 g, 3.85 mmol of pentafluorophenyl functionalities, 1.0 equiv, $M_w = 7900$, $M_w/M_n = 2.8$, from GPC based upon PS standards) by the same procedure as for the preparation of **4**. The product was purified twice by silica flash chromatography using 80% hexane/acetone to give **6** as a colorless glass, containing 95–100% of the chain ends substituted by the perfluorodecanoxy group, by ¹⁹F NMR: yield 1.50 g (43%); $M_w = 33\,000$, $M_w/M_n = 5$, from GPC based upon PS standards; $T_g = 54$ °C; IR 3100–2900, 1656, 1599, 1500, 1467, 1378, 1291, 1242, 1214, 1153, 1057, 1006, 941, 828, 730, 692 cm⁻¹; ¹H NMR (CDCl₃) δ 2.65 (br m, 2H, CF₃(CF₂)₇CH₂CH₂O), 4.53 (br m, 2H, CF₃(CF₂)₇CH₂CH₂O), 5.05 (br s, 4H, C₆F₄CH₂O), 5.19 (br s, 2H, ArCH₂O), 6.53 (br m, 1H, ArH), 6.70 (br m, 2H, ArH) ppm; ¹³C NMR (CDCl₃) δ 31.9 (t, $J = 17$ Hz, aliphatic CF₂CH₂), 57.6 (C₆F₄CH₂O), 57.7 (C₆F₄CH₂O), 66.8 (aliphatic CH₂O), 75.9 (ArCH₂O), 102.5 (ArCH), 107.3 (ArCH), 108.6 (m,

tetrafluorophenyl *ipso*-C), 109.4 (m, CF₃), 109.9 (m, tetrafluorophenyl *ipso*-C), 110.3 (m, aliphatic CF₂), 110.9 (m, aliphatic CF₂), 111.5 (m, aliphatic CF₂), 117.3 (m, aliphatic CF₂), 136.5 (m, tetrafluorophenyl *ipso*-C), 137.6 (m, tetrafluorophenyl *ipso*-C), 138.4 (Ar *ipso*-C), 140.9 (d of m, *J* = 250 Hz, ArCF), 141.2 (d of m, *J* = 250 Hz, ArCF), 145.8 (d of m, *J* = 250 Hz, ArCF), 159.3 (s, Ar *ipso*-C), 159.5 (s, Ar *ipso*-C) ppm; ¹⁹F NMR (CDCl₃) δ -81.3 (s, 3F, aliphatic CF₃), -113.8 (s, 2F, aliphatic CF₂), -122.4 (s, 6F, aliphatic CF₂), -123.2 (s, 2F, aliphatic CF₂), -124.0 (s, 2F, aliphatic CF₂), -126.6 (s, 2F, aliphatic CF₂), -144.1 (m, 2F, C₆F₄ArF), -144.4 (m, 2F, C₆F₄ArF), -156.5 (m, 2F, C₆F₄ArF), -157.2 (m, 2F, C₆F₄ArF) ppm. Anal. Calcd for 100% repeat unit of C₃₁H₁₃F₂₅O₄ (924.40): C, 40.28; H, 1.42; F, 51.38. Found: C, 40.99; H, 1.36; F, 46.23.

***p*-Iodophenoxy-Substituted 2 (7).** A mixture of **2** (0.20 g, 0.42 mmol of pentafluorophenyl functionalities) and *p*-iodophenol (0.092 g, 0.42 mmol) was allowed to react with K₂CO₃ (0.064 g, 0.46 mmol, 1.1 equiv) and 18-crown-6 (ca. 0.1 equiv) in DMF (5 mL) with stirring at room temperature under Ar for 3 days. The reaction mixture was concentrated in vacuo and redissolved into CH₂Cl₂, and the product was purified twice by silica flash chromatography using 70% hexanes/CH₂Cl₂, increasing to CH₂Cl₂, as eluent to give **7** as a transparent glass, containing 90% substitution of the *p*-fluorine atoms, from ¹⁹F NMR: yield 0.095 g (35%); IR 3100–2900, 1656, 1598, 1499, 1480, 1429, 1378, 1297, 1208, 1169, 1057, 1007, 981, 940, 823, 734 cm⁻¹; ¹H NMR (CDCl₃) δ 5.06 (br s, 2H, IArO–C₆F₄CH₂O), 5.13 (br s, 2H, C₆F₄CH₂O), 5.20 (br s, 2H, ArCH₂O), 6.5–6.8 (br m, 3H, ArH), 6.74 and 7.60 (ABq, 4H, *J* = 8 Hz, IArH) ppm; ¹³C NMR (CDCl₃) δ 57.7 (s, C₆F₄CH₂O), 75.9 (ArCH₂O), 86.8 (Ar *ipso*-C), 101.3 (ArCH), 102.4 (ArCH), 106.1 (tetrafluorophenyl *ipso*-C), 107.3 (tetrafluorophenyl *ipso*-C), 117.8 (ArCH), 128.8 (tetrafluorophenyl *ipso*-C), 130.9 (tetrafluorophenyl *ipso*-C), 138.7 (ArCH), 140.8 (d of m, *J*_{C–F} = 250 Hz, ArCF), 145.7 (d of m, *J*_{C–F} = 250 Hz, ArCF), 156.9 (Ar *ipso*-C), 158.4 (Ar *ipso*-C) ppm; ¹⁹F NMR (CDCl₃) δ -142.9 (m, 2F, ArF), -144.3 (m, 2F, ArF), -154.1 (m, 2F, ArF), -156.4 (m, 2F, ArF) ppm. Anal. Calcd 90% repeat units C₂₇H₁₃F₈I₂O₄ (680.29), 10% repeat units C₂₁H₉F₉O₃ (480.28): C, 48.16; H, 1.93; F, 23.67; I, 16.79. Found: C, 46.81; H, 2.05; F, 18.36; I, 20.29.

Conclusion

A highly branched polymer containing perfluoroaromatic rings throughout the structure has been synthesized. The molecular weight of the polymer can be easily varied. Derivatization of the initial material is accomplished by nucleophilic aromatic substitution of the *p*-fluorine of the pentafluorophenyl chain ends. All polymers are highly soluble in organic solvents and are highly hydrophobic. Atomic force microscopy (AFM) is proving useful in the characterization of the surface morphologies and the coefficients of friction for these highly branched polymers. Additionally, the micromechanical properties of the materials are currently under investigation using AFM.

Potential uses for these materials include lubricants and coatings in applications that require minimally adhesive materials. The chemical inertness of fluoropolymers is desirable in their application as engineering materials; however, this also leads to difficulties in chemical modification of their surfaces.²⁵ In the case of the hyperbranched polymers, reactive chain ends, which offer sites that can be consumed for surface or bulk modification, remain after the polymerization.

Acknowledgment. Financial support for this work from the U.S. Army Research Office, Young Investigator Award Program (DAAH 04-96-1-0158) (K.L.W.), the National Science Foundation, Young Investigator Award Program (DMR-9458025) (K.L.W.), and the Office of

Naval Research (T.K.) is gratefully acknowledged. The authors thank André d'Avignon of the Washington University High Resolution NMR Service Facility, funded in part by the National Institutes of Health (Grants 1S10RR02204 and RR05018) and the National Science Foundation (Grants CHE-9319666), for assistance with ¹⁹F-decoupled ¹³C NMR. The authors also thank Pierangelo Groening (U. Fribourg, Switzerland) and Professor Rodney Ruoff (Washington University, Department of Physics) for making available the Teflon-coated Si wafer and Dr. Andrei Stefanescu for ¹⁹F NMR calculations of molecular weights.

References and Notes

- (1) For several reviews on this subject see: (a) Fréchet, J. M. J. *Science* **1994**, *263*, 1710. (b) Ardoin, N.; Astruc, D. *Bull. Soc. Chim.* **1995**, *132* (9), 875. (c) Voit, B. I. *Acta Polym.* **1995**, *46*, 87. (d) Dvornic, P. R.; Tomalia, D. A. *Curr. Opin. Colloid Interface Sci.* **1996**, *1* (2), 221. (e) *Advances in Dendritic Molecules*; Newkome, G. R., Ed.; JAI Press: Greenwich, CT, 1994–5; Vol. 1–2. (f) Newkome, G. R.; Moorefield, C. N.; Vögtle, F. *Dendritic Molecules, Concepts, Syntheses, Perspectives*; VCH Publishers, Inc.: New York, 1996.
- (2) Mourey, T. H.; Turner, S. R.; Rubinstein, M.; Fréchet, J. M. J.; Hawker, C. J.; Wooley, K. L. *Macromolecules* **1992**, *25*, 240.
- (3) Hawker, C. J.; Farrington, P. J.; Mackay, M. E.; Wooley, K. L.; Fréchet, J. M. J. *J. Am. Chem. Soc.* **1995**, *117*, 4409.
- (4) Wooley, K. L.; Klug, C. A.; Tasaki, K.; Schaefer, J. *J. Am. Chem. Soc.* **1997**, *119*, 53.
- (5) (a) Mansfield, M. L. *Polymer* **1994**, *35* (9), 1827–30. (b) Mansfield, M. L. *Polymer* **1996**, *37* (17), 3835–41.
- (6) Hawker, C. J.; Malmström, E. E.; Frank, C. W.; Kampf, J. P. *J. Am. Chem. Soc.* **1997**, *119*, 9903.
- (7) Wooley, K. L.; Fréchet, J. M. J.; Hawker, C. J. *Polymer* **1994**, *35* (21), 4489.
- (8) (a) Wang, J.; Mao, G.; Ober, C. K.; Kramer, E. J. *Macromolecules* **1997**, *30*, 1906. (b) Wang, W.; Castner, D. G.; Grainger, D. W. *Supramol. Sci.* **1997**, *4*, 83. (c) Schnurrer, A. U.; Holcomb, N. R.; Gard, G. L.; Castner, D. G.; Grainger, D. W. *Chem. Mater.* **1996**, *8*, 1475–81. (d) Smith, D. W., Jr.; Babb, D. A. *Macromolecules* **1996**, *29*, 852. (e) Schmidt, D. L.; DeKoven, B. M.; Coburn, C. E.; Potter, G. E.; Meyers, G. F.; Fischer, D. A. *Langmuir* **1996**, *12*, 518. (f) Zhang, Y.-X.; Da, A.-H.; Butler, G. B.; Hogen-Esch, T. E. *J. Polym. Sci., Polym. Chem. Ed.* **1992**, *30*, 1383. (g) Irvin, J. A.; Neef, C. J.; Kane, K. M.; Cassidy, P. E.; Tullios, G.; St. Clair, A. K. *J. Polym. Sci., Polym. Chem. Ed.* **1992**, *30*, 1675–9.
- (9) Chambers, R. D. *Fluorine in Organic Chemistry*; Olah, G. A., Ed.; Interscience Monographs on Organic Chemistry; John Wiley & Sons: New York, 1973.
- (10) (a) Smart, B. E. In *Organofluorine Chemistry, Principles and Commercial Applications*; Banks, B. E., Smart, B. E., Tatlow, J. C., Eds.; Plenum Press: New York and London, 1994; pp 57–88. (b) Brady, R. F. *Chem. Br.* **1990**, 427. (c) Gangal, S. V. In *Encyclopedia of Polymer Science and Engineering*; Mark, H. F., Bikales, N. M., Overberger, C. G., Menges, G., Eds.; Wiley Interscience: New York, 1989; Vol. 16, pp 677–9.
- (11) (a) Chu, F.; Hawker, C. J. *Polym. Bull.* **1993**, *30*, 256. (b) Miller, T. M.; Neenan, T. X.; Kwock, E. W.; Stein, S. M. *J. Am. Chem. Soc.* **1993**, *115*, 356. (c) Miller, T. M.; Neenan, T. X.; Zayas, R.; Bair, H. E. *J. Am. Chem. Soc.* **1992**, *114*, 1018.
- (12) Straw, T. S.; Kowalewski, T.; Wooley, K. L. Manuscript in preparation.
- (13) (a) Carter, K. *Macromolecules* **1995**, *28*, 6462. (b) Hendricks, N. H.; Lau, K. S. Y. *ACS Polym. Prepr.* **1996**, *37* (1), 150.
- (14) (a) Weiss, R.; Pomrehn, B.; Hampel, F.; Bauer, W. *Angew. Chem., Int. Ed. Engl.* **1995**, *34*, 4 (12), 1319–21. (b) Wall, L. A.; Pummer, W. J.; Fearn, J. E.; Antonucci, J. M. *J. Res. Natl. Bur. Std.* **1963**, *67A*, 481.
- (15) Hölter, D.; Burgath, A.; Frey, H. *Acta Polym.* **1997**, *48*, 30.
- (16) Sammes, P. G.; Thetford, D.; Voyle, M. *J. Chem. Soc., Perkin Trans. 1* **1988**, 3229–31.
- (17) Neumann, A. W.; Good, R. J. *Surf. Colloid Sci.* **1979**, *11*, 31.
- (18) Zhong, Q.; Inniss, D.; Kjoller, K.; Ellings, V. B. *Surf. Sci.* **1993**, *290*, L688.
- (19) Kowalewski, T.; Schaefer, J. *PMSE Prep.* **1997**, *76*, 215.

- (20) Percec, V.; Johansson, G.; Ungar, G.; Zhou, J. *J. Am. Chem. Soc.* **1996**, *118*, 9885.
- (21) (a) Binnig, G.; Quate, C. F.; Gerber, C. *Phys. Rev. Lett.* **1986**, *56*, 930. (b) Meyer, G.; Amer, N. M. *Appl. Phys. Lett.* **1988**, *52*, 1045. (c) Meyer, G.; Amer, N. M. *Appl. Phys. Lett.* **1990**, *57*, 2089.
- (22) Ruan, J.-A.; Bhushan, B. *J. Tribol.* **1994**, *116*, 378.
- (23) Digital Instruments, Santa Barbara, CA (<http://www.di.com>).
- (24) Tsukruk, V. V.; Bliznyuk, V. N.; Wu, J.; Visser, D. W. *Polym. Prepr.* **1996**, *37* (2), 575–6.
- (25) Kang, E. T.; Tan, K. L.; Kato, K.; Uyama, Y.; Ikada, Y. *Macromolecules* **1996**, *29*, 6872.

MA971201Z